Global sensitivity and uncertainty analysis of an atmospheric chemistry transport model: the FRAME model (version 9.15.0) as a case study

5   Ksenia Aleksankina,[1,2] Mathew R. Heal,[1] Anthony J. Dore,[2] Marcel Van Oijen,[2] Stefan Reis[2,3]

[1] School of Chemistry, University of Edinburgh, Edinburgh, UK
[2] NERC Centre for Ecology & Hydrology, Penicuik, UK
[3] University of Exeter Medical School, European Centre for Environment and Health, Knowledge Spa, Truro, UK

Correspondence to: Mathew Heal (m.heal@ed.ac.uk)

Abstract. Atmospheric chemistry transport models (ACTMs) are widely used to underpin policy decisions associated with the impact of potential changes in emissions on future pollutant concentrations and deposition. It is therefore essential to have a

15   quantitative understanding of the uncertainty in model output arising from uncertainties in the input pollutant emissions. ACTMs incorporate complex and non-linear descriptions of chemical and physical processes which means that interactions and non-linearities in input–output relationships may not be revealed through the local one-at-a-time sensitivity analysis typically used. The aim of this work is to demonstrate a global sensitivity and uncertainty analysis approach for an ACTM, using as an example the FRAME model, which is extensively employed in the UK to generate source-receptor matrices for

20   the UK Integrated Assessment Model and to estimate critical load exceedances. An optimised Latin hypercube sampling design was used to construct model runs within $\pm$ 40 % variation range for the UK emissions of SO_2, NO_x and NH_3, from which regression coefficients for each input-output combination and each model grid (>10,000 across the UK) were calculated. Surface concentrations of SO_2, NO_x and NH_3 (and of deposition of S and N) were found to be predominantly sensitive to the emissions of the respective pollutant, while sensitivities of secondary species such as HNO_3 and particulate SO_4^{2-}, NO_3^- and

25   NH_4^+ to pollutant emissions were more complex and geographically variable. The uncertainties in model output variables were propagated from the uncertainty ranges reported by the UK National Atmospheric Emissions Inventory for the emissions of SO_2, NO_x and NH_3 ($\pm$ 4 %, $\pm$ 10 % and $\pm$ 20 % respectively). The uncertainties in the surface concentrations of NH_3 and NO_x and the depositions of NH_x and NO_y were dominated by the uncertainties in emissions of NH_3, and NO_x respectively, whilst concentrations of SO_2 and deposition of SO_y were affected by the uncertainties in both SO_2 and NH_3 emissions. Likewise, the

30   relative uncertainties in the modelled surface concentrations of each of the secondary pollutant variables (NH_4^+, NO_3^-, SO_4^{2-} and HNO_3) were due to uncertainties in at least two input variables. In all cases the spatial distribution of relative uncertainty was found to be geographically heterogeneous. The global methods used here can be applied to conduct sensitivity and uncertainty analyses of other ACTMs.

1 Introduction

Atmospheric chemistry transport models (ACTMs) provide scientific support for policy development. It is therefore important to have a quantitative understanding of the levels of uncertainty associated with model outputs (AQEG, 2015; Frost et al., 2013; Rypdal and Winiwarter, 2001). Sensitivity and uncertainty analyses are both used in this regard. Uncertainty analysis is applied to quantify propagation of uncertainties of single or multiple inputs through to a model output, whilst sensitivity analysis is used to investigate input-output relationships and to apportion the variation in model output to the different inputs. However, due to the complexity of ACTMs the relationship between model inputs and outputs is not analytically tractable so both quantities must be estimated by sampling model inputs according to an experimental design and undertaking multiple model simulations (Dean et al., 2015; Norton, 2015; Saltelli et al., 2000; Saltelli and Annoni, 2010).

Typically, model assessment studies focus on uncertainties in the model parameter values (Derwent, 1987; Konda et al., 2010; De Simone et al., 2014) and model-specific structure (Simpson et al., 2003; Thompson and Selin, 2012). However, for ACTMs the uncertainty in the model input emissions data could be dominating; for example, previous dispersion model uncertainty studies identified input emissions as a primary source of uncertainty in model outputs (Bergin et al., 1999; Hanna et al., 2007; Sax and Isakov, 2003). It is also the case that a major role of ACTMs is to estimate the impact of potential future changes in emissions on atmospheric composition (Boldo et al., 2011; Crippa et al., 2016; Heal et al., 2013; Vieno et al., 2016; Xing et al., 2011; Zhang et al., 2010).

Thus the focus of this study is to demonstrate a systematic approach for quantifying model output sensitivity and uncertainty as a function of the variation in model input emissions. We used the Fine Resolution Atmospheric Multi-pollutant Exchange (FRAME) model as a case study. FRAME is a Lagrangian model that outputs, at a 5 km × 5 km horizontal resolution over the UK, annual average surface concentrations of sulphur dioxide (SO_2), nitrogen oxides (NO_x), ammonia (NH_3), nitric acid (HNO_3), and particulate ammonium (NH_4^+), sulphate (SO_4^{2-}), and nitrate (NO_3^-), together with dry and wet deposition of oxidised sulphur (SO_y), oxidised nitrogen (NO_y), and reduced nitrogen (NH_x) (Dore et al., 2012; Matejko et al., 2009; Singles et al., 1998). The model is extensively used to provide policy support including generation of source-receptor matrices for the UK Integrated Assessment Model (UKIAM) and estimation of critical load exceedances (Matejko et al., 2009; Oxley et al., 2013). Source receptor matrices link concentration and deposition with individual emission sources and are used to automate procedures to estimate the impact of future emission reduction scenarios. Integrated assessment modelling incorporates technical emissions abatement costs with cost-benefit analysis and source-receptor data to indicate cost-effective solutions to protect natural ecosystems from acidic and nitrogen deposition above defined critical thresholds and to protect human health from particulate concentrations (Oxley et al., 2003, 2013).

FRAME uses emissions input data from the UK National Atmospheric Emissions Inventory (NAEI, http://naei.beis.gov.uk/), which are compiled following the international 'Guidelines for Reporting Emissions and Projections Data under the

Convention on Long-range Transboundary Air Pollution (United Nations Economic Commission for Europe, 2015). We used the uncertainties published by the NAEI in the Informative Inventory Report (Misra et al., 2015) as the foundation of the uncertainty propagation for the FRAME concentration and deposition outputs with respect to UK emissions of SO_2, NO_x, and NH_3. The uncertainty ranges for different pollutants reported by the NAEI are estimated using a Monte Carlo technique which

5   corresponds to the IPCC Tier 2 approach (IPCC, 2006). In this approach uncertainty ranges for each source for both emission factor and activity statistics are associated with a probability distribution and further used as inputs in a stochastic simulation which calculates output distributions of total UK emissions for each pollutant. The uncertainties are expressed as plus or minus half the confidence interval width relative to the estimated emissions value.

Previously, local one-at-a-time (OAT) sensitivity analysis has been used to investigate ACTM sensitivity because it is less

10   computationally demanding than global sensitivity analysis that requires a large number of simultaneous perturbations of all inputs of interest. However, there are significant disadvantages associated with OAT analysis: the interactions between the input parameters and non-linearities in the model response cannot be identified; additionally as the number of input parameters increases the fraction of parameter space investigated tends to zero (Jimenez and Landgrebe, 1998; Saltelli and Annoni, 2010). Therefore local OAT sensitivity analysis is only applicable when the effects of the different inputs are all independent from

15   each other and model response is linear for the range of investigated inputs. Many previous publications that include ACTM sensitivity analysis use the OAT approach but fail to acknowledge its limitations (Appel et al., 2007; Borge et al., 2008; Capaldo and Pandis, 1997; Labrador et al., 2005; Makar et al., 2009).

Hence this study focuses on demonstrating the use of global methods capable of revealing non-linearity in the model response and the presence of interactions between inputs in addition to revealing the spatial pattern of the model response to changes in

20   the input emissions. Global sensitivity and uncertainty analyses have been applied in many earth science fields such as hydrological modelling (Shin et al., 2013; Yatheendradas et al., 2008), ecological modelling (Lagerwall et al., 2014; Makler-Pick et al., 2011; Song et al., 2012), and atmospheric aerosol modelling (Carslaw et al., 2013; Chen et al., 2013; Lee et al., 2011). Increasing computational resource means this approach is now starting to be applied to ACTMs (Christian et al., 2017). In a global sensitivity analysis a sample space is created for all inputs under investigation from which a set of combinations of

25   model inputs for different model runs are chosen. The sampling design for model inputs for uncertainty and sensitivity analysis must balance the needs of covering the full multidimensional input parameter space at sufficient density to allow characterisation of any non-linearities and interactions in the model response with a small enough number of samples for the total number of model runs to remain computationally tractable. Simple random sampling is conceptually the simplest sampling technique, but has low efficiency compared to other sampling approaches and tends to lead to clusters and gaps in

30   coverage of the input space (Saltelli et al., 2008). Likewise, full or fractional factorial designs (Box and Hunter, 1961) do not allow effective exploration of the whole input space because for more than a few levels of each input the number of model runs becomes very large. Quasi-random sampling, of which the Sobol' sequence (Sobol', 1967, 1976; Sobol' and Levitan, 1999) is a popular choice for variance-based sensitivity analysis, may not work well when the number of sampling points is small (Saltelli et al., 2008). Therefore, in this work, Latin hypercube sampling (LHS) (McKay et al., 1979), which is a stratified

space-filling sampling technique, was used. Advances have been made to optimise the space filling properties of LHS including maximin sampling (Johnson et al., 1990; Morris and Mitchell, 1995) and integrated mean squared-error minimisation (Park, 1994).

In summary, this work demonstrates application of global uncertainty and sensitivity analysis to an ACTM using the FRAME
5   model as an example.

2 Methods

2.1 Model description

The FRAME model is a Lagrangian model that calculates annual average surface concentrations of SO_2, NO_x, NH_3, and HNO_3, particulate NH_4^+, SO_4^{2-}, and NO_3^-, and dry and wet deposition of SO_y, NO_y and NH_x at 5 km × 5 km horizontal resolution over
10   the UK (Dore et al., 2012; Fournier et al., 2002; Matejko et al., 2009; Singles et al., 1998). This spatial resolution corresponds to >10,000 model grid squares over the UK land area. The air column contains 33 vertical layers of varying thickness from 1 m at the surface to 100 m at the top of the mixing layer. The vertical diffusion between layers is calculated using *K*-theory. The air columns move from the boundary of the domain along straight-line trajectories with varying starting angles at a 1° resolution. The trajectories are defined by an annual wind rose and annually-averaged wind speed generated for year 2012
15   from the output of the Weather Research and Forecast model (www.wrf-model.org) (Skamarock et al., 2008) version 3.7.1. The model was run at a 5 km resolution over the UK with boundary and initial conditions initialised by the National Centers for Environmental Prediction Final Global Forecast System (NCEP-GFS-FNL) data (https://rda.ucar.edu/datasets/ds083.2/). Gridded emissions of SO_2, NO_x, and NH_3 are obtained from the UK NAEI (http://naei.beis.gov.uk/) at 1 km × 1 km spatial resolution (maps are shown in Figure S1 in Supplementary Information). Input emissions of SO_2 and NO_x are split into three
20   categories: UK area, point source, and shipping emissions. FRAME treats SO_2 emissions as 95% SO_2 and 5% H_2SO_4, and NOx emissions as 95% NO and 5% NO_2. For NH_3 emissions there are only UK area and point source categories. The NH_3 emissions from livestock are distributed spatially according to Hellsten et al. (2008). All emissions are injected into the air column at different heights according to the classification of emission sources.

The chemical scheme is described in Fournier et al. (2004) and includes gaseous and aqueous-phase oxidation reactions and
25   conversion of the gases NH_3, SO_2, and NO_x to particulate matter (NH_4^+, NO_3^-, SO_4^{2-}). NH_4NO_3 is formed by the equilibrium reaction between HNO_3 and NH_3 and nitrate aerosol also arises by the deposition of HNO_3 onto sea salt or large particles. H_2SO_4 reacts with NH_3 to form $(NH_4)_2SO_4$. The aqueous phase reactions include the oxidation of S(IV) by O_3 and the metal catalysed reaction with O_2. Modelled dry deposition is land-cover dependent and calculated using a canopy resistance model. Wet deposition is calculated using scavenging coefficients and it is driven by rainfall, which is modelled using a constant
30   drizzle approach based on the measured spatial distribution of annual average rainfall data with the assumption of an enhanced washout rate over elevated areas.

A detailed evaluation of model outputs with annually averaged measurements of pollutant concentrations in air and precipitation concentrations is discussed elsewhere (Dore et al., 2015). In this study, all model runs were performed using emissions and meteorology data for the year 2012 and FRAME model version 9.15.0.

2.2 Sensitivity and uncertainty analysis

5   For both sensitivity and uncertainty analyses a Latin hypercube sampling design was chosen as it is superior to quasi-random sampling for small numbers of samples (Saltelli et al., 2008). A uniform LHS design was created using the R package 'lhs'(Carnell, 2016), with the sample optimised by maximising the mean distance between the design points. The LHS design was created for the scaling coefficients applied to the model input emissions of UK SO_2, NO_x and NH_3 and not for the actual values of the input emissions. This means that emissions from all sources of a particular pollutant were varied by the same

10   fraction across all grid squares in a particular model run.

For the sensitivity analysis a uniform LHS sample of size $n = 100$ within a range of ± 40 % relative to the baseline for each of the three input variables was created. This range was chosen to test the overall model response to changes in emissions (for example to identify non-linearities) as it encompasses the range of variations in input emissions used for future scenario simulations with the FRAME model, as well as incorporating emission reductions applied for the generation of source-receptor

15   relationships for integrated assessment modelling.

Regression coefficients (RC) were used as the measure of the sensitivity of the model response, derived as follows. For each model grid cell, and for each model output variable, a multiple linear regression (Eq. 1) was performed using the data from the $n = 100$ model runs. To obtain the RCs (b_i in Eq. 1) the model inputs X_i, and outputs Y, were substituted by corresponding values of fractional change relative to the baseline value. This simplifies interpretation of the resulting RCs. A RC represents

20   the relative effect of changing input X_i on the output Y, e.g. RC = 0.5 signifies a 15 % reduction in the output variable value if an input is reduced by 30 %. The coefficients of determination (R^2) were evaluated for each fitted model (for every grid cell) to identify if a significant level of non-linearity in the input-output relationship was present.

$$Y = b_0 + \sum_{i=1}^{3} b_i X_i \tag{1}$$

For the uncertainty propagation, the input sampling space was constrained to the specific uncertainty ranges assigned to the emissions of SO_2, NO_x and NH_3 in the UK Informative Inventory Report (Misra et al., 2015) with a new LHS sample $n = 100$.

25   These uncertainty ranges are derived following published guidelines on quantifying uncertainties in emissions estimates (IPCC, 2006; Pulles and Kuenen, 2016). According to the guidelines, uncertainties are expressed as lower and upper limits of the 95 % confidence interval as a percentage of the central estimate. The assigned emissions uncertainties have ± 4 %, ± 10 % and ± 20 % ranges, for SO_2, NO_x and NH_3 respectively. The probability distributions were not specified, therefore it was chosen to use uniform distributions for the variable ranges from which the LHS sample was created. It is also acknowledged

30   that a number of other aspects of emissions uncertainty are not included. For example, the FRAME model cannot capture

uncertainty in assigned seasonal and diurnal cycles in emissions. Uncertainties in the spatial distributions or in height of elevated emissions are also not included.

The uncertainty values for each grid square were calculated as a half of the 95% confidence interval relative to the mean value of the output as recommended in the EMEP/EEA and IPCC Guidebooks (IPCC, 2006; Pulles and Kuenen, 2016). Relative uncertainty values are presented here.

To assess the contribution of uncertainties in the emissions of SO_2, NO_x and NH_3 to the overall output uncertainty standardised regression coefficients (SRCs) were calculated as shown in Eq. 2. A multiple linear regression was performed using the data from the 100 model simulations for the case of constrained input sampling space. The SRCs (β_i in Eq. 2) were calculated by multiplying the RC by the ratio between the standard deviations of the input σ_i, and output σ_Y. (σ_Y is the same for all the β_i values for a given output variable.)

$$\beta_i = b_i \frac{\sigma_i}{\sigma_Y} \tag{2}$$

The squared value of SRC (Eq. 3) for linear additive models is equal to the ratio of variance of mean of Y when one input variable is fixed, $V_{X_i}(E_{X_{\sim i}}(Y|X_i))$, to the unconditional variance of Y, $V(Y)$ (Saltelli et al., 2008). Thus SRC squared represents the fractional contribution of the uncertainties in the model inputs to the overall uncertainty in the output. For the case of non-linear models, variance decomposition methods are described in more detail elsewhere (Homma and Saltelli, 1996; Saltelli, 2002; Saltelli et al., 2010; Sobol', 1993). In the case where a large number of model simulations is not possible an emulator based approach can be used for the uncertainty and sensitivity analysis (Blatman and Sudret, 2010; Lee et al., 2011; Shahsavani and Grimvall, 2011; Storlie and Helton, 2008).

$$\beta_i^2 = \frac{V_{X_i}(E_{X_{\sim i}}(Y|X_i))}{V(Y)} \tag{3}$$

3 Results and discussion

3.1 Global sensitivity analysis

Figure 1 summarises the distributions of the regression coefficient (RC) global sensitivity measure across all model grid cells. RCs show the sensitivity of each model output variable to the three input emissions variables (SO_2, NO_x and NH_3), and can be interpreted as a magnitude of the response of an output to the unit change in a particular input when all other inputs are allowed to vary. The magnitude of the RCs provides useful information not only about the effect of the change in a particular input on a model output, but also allows input sensitivity ranking to be determined because all inputs were assigned the same range of variation ($\pm$ 40 %). In the case where the ranges for inputs differ, standardised regression coefficients (SRCs) are used to obtain the input importance ranking instead.

Figure 1 shows that model outputs have (i) varying sensitivities, (ii) varying relative rankings in their sensitivities to SO_2, NO_x and NH_3 emissions, and (iii) that these output sensitivities to the emissions also vary spatially across the model grids, as shown

by the spreads in individual box plots. The annual average concentrations of particulate NH_4^+, NO_3^-, and SO_4^{2-} and annual dry and wet deposition of SO_y for the baseline model run are presented in Supplementary Information Figure S2. The actual spatial distributions of the RCs from Figure 1 are illustrated in Figure 2 for the example output variables of particulate NH_4^+, NO_3^-, and SO_4^{2-}. Figure 3 shows the equivalent for the example output variables of dry and wet deposition of SO_y. These five output

5   variables were chosen to illustrate the spatial distribution of uncertainty and sensitivity metrics. Figures S3 and S4 in Supplementary Information show the spatial distribution of RCs for other FRAME outputs displayed in Figure 1.

RC is a first-order sensitivity measure and it quantifies the average response of model output to varying a model input X_i when all inputs are allowed to vary. In this study no second, or higher, order interaction terms were quantified as their contribution was assumed to be negligible. This was concluded from the values of the coefficients of determination (R^2) obtained from

10   multiple linear regressions performed; for most output variables, values of R^2 were on average > 0.98 with the exception of a slightly lower value for HNO_3 (R^2 > 0.96). Hence less than 2 % (4 % for HNO_3) of variance in the output could not be explained by the linear combination of inputs. This finding allows us to conclude that the FRAME model response is in fact fairly linear within the ± 40 % emission perturbation range investigated. The absence of any substantial deviations from linearity in the model response and absence of second or higher order interactions between input variables indicate that the current use of the

15   FRAME model to produce source-receptor matrices for the use in the UK Integrated Assessment Model is not subject to undue error from varying emissions one-at-a-time. Without conducting the global sensitivity analysis it is not possible to predict a priori for a given model output variable either the relative sensitivities to the different input factors, such as emissions, or the spatial variation in these sensitivities that are illustrated in Figures 1, 2 and 3.
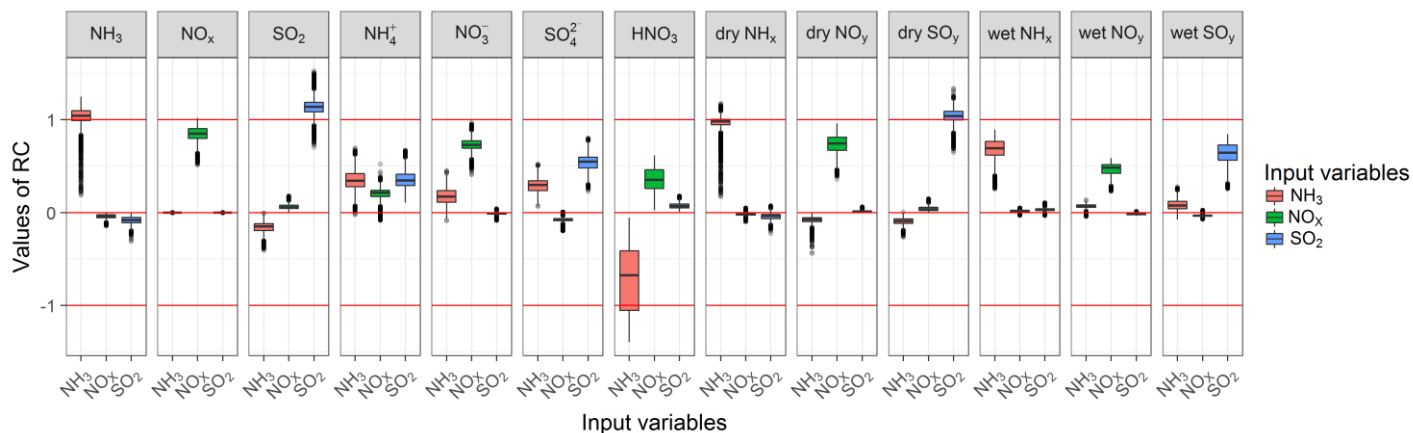
20   **Figure 1 Box plots of the values of regression coefficients (RC) across all UK land-based model grid squares. Boxes demarcate the median and lower/upper quartiles of the distributions; whiskers extend to 1.5 times the interquartile range.**
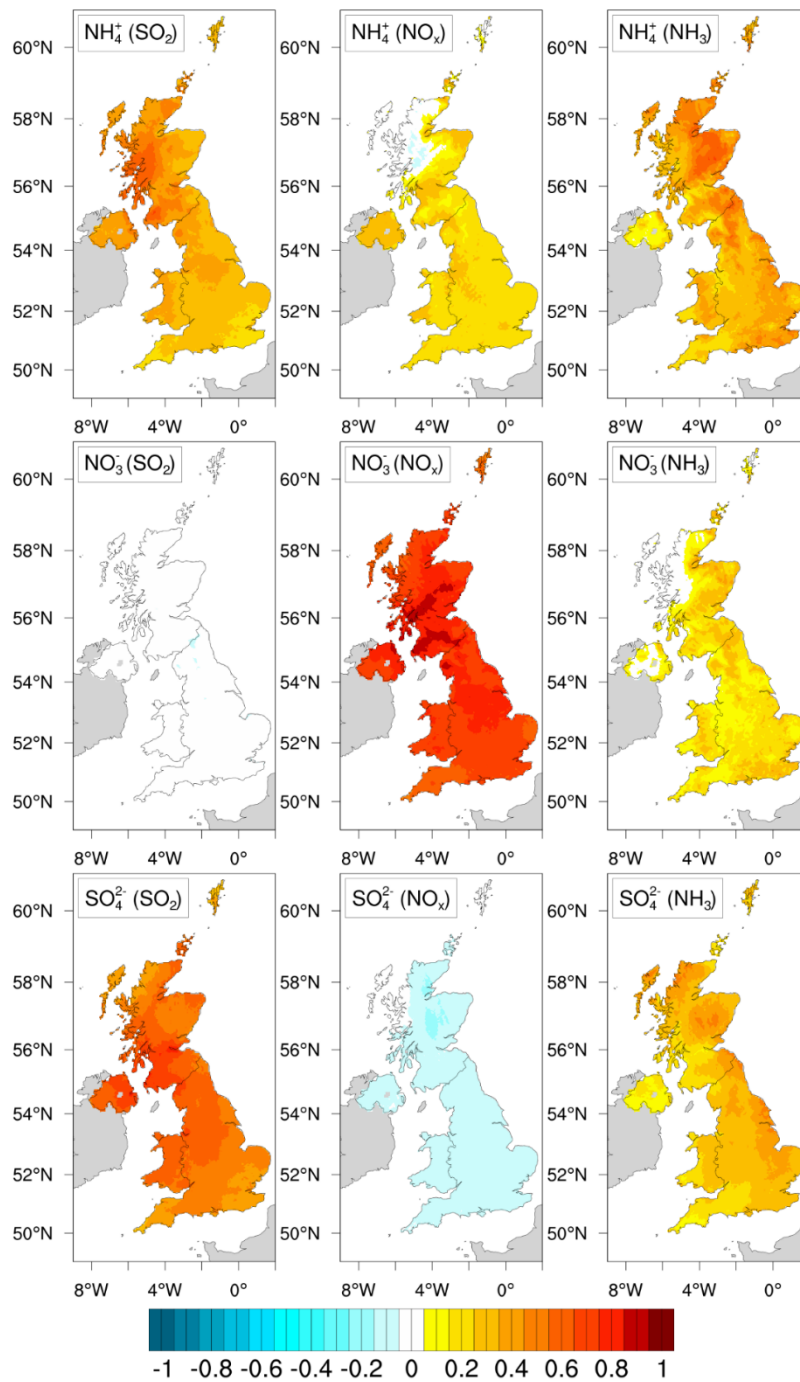
Figure 2 Spatial distributions (at the 5 km × 5 km model grid resolution) of RCs for particulate NH$_4^+$, SO$_4^{2-}$, and NO$_3^-$ as a function of variation in input emissions of SO$_2$, NO$_x$ or NH$_3$. The model input emissions for which the RC quantifies the output variable sensitivity is given in brackets in each panel.
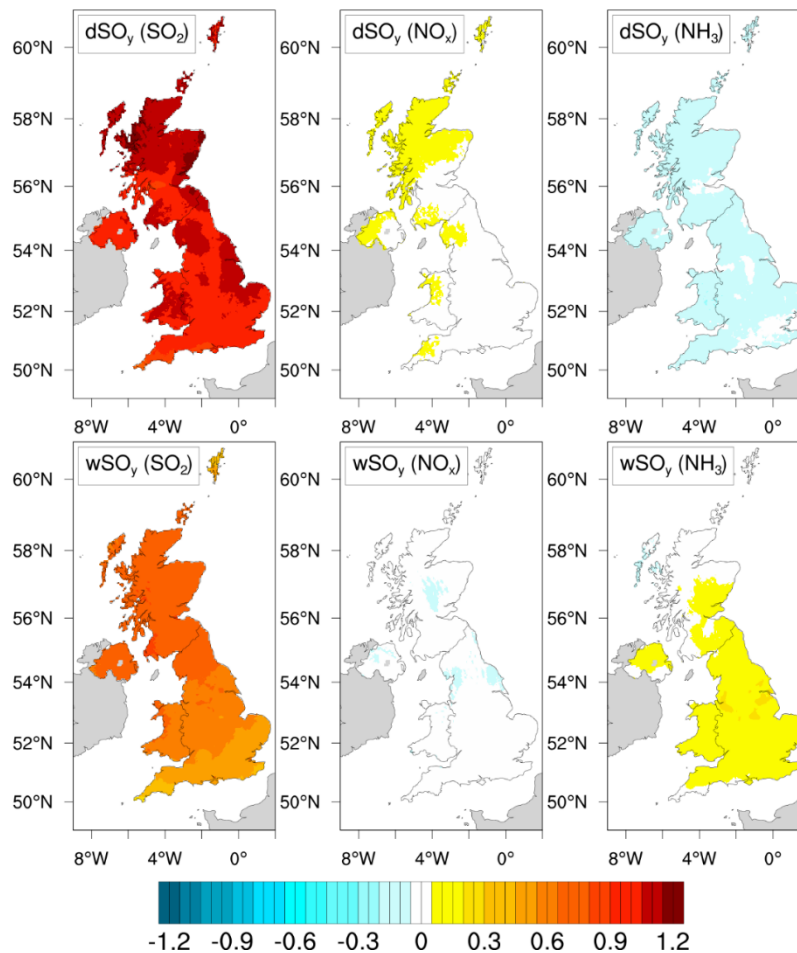
Figure 3 Spatial distributions (at the 5 km × 5 km model grid resolution) of RCs of dry (d) and wet (w) deposition of SO$_y$ as a function of variation in input emissions of SO$_2$, NO$_x$ or NH$_3$. The model input emissions for which the RC quantifies the output variable sensitivity is given in the brackets in each panel.

With respect to findings from this FRAME model sensitivity analysis for particulate inorganic components in the UK context, Figure 1 shows that the modelled surface concentrations of particulate NH$_4^+$ are sensitive to changes in emissions of all three pollutants, being similarly sensitive (on average) to emissions of NH$_3$ and SO$_2$, and slightly less sensitive to emissions of NO$_x$. The sensitivities of NH$_4^+$ to SO$_2$, NO$_x$ and NH$_3$ emission changes were found to vary substantially around the UK (top row of

10 Figure 2). Sensitivity of NH$_4^+$ to SO$_2$ emissions is generally lowest in south-east England, and rises on moving north and west across the UK. Reductions in emissions are always associated with reductions in NH$_4^+$. The broad geographical pattern of relative sensitivity across the UK of NH$_4^+$ to NH$_3$ emissions is approximately the reverse of that to SO$_2$ emissions although with substantial spatial heterogeneity as well. Figure 2 shows that there are instances in north-west Scotland of negative RCs for the sensitivity of NH$_4^+$ to NO$_x$ emissions, i.e. areas where NH$_4^+$ increases when NO$_x$ emissions are decreased.

Figure 1 similarly shows that surface concentrations of particulate SO_4^{2-} are sensitive to changes in emissions of all three of SO_2, NO_x and NH_3 (most sensitive to SO_2 emissions) but with a universally negative sensitivity (albeit relatively weak) to NO_x emissions, i.e. particulate SO_4^{2-} concentrations increase everywhere by approximately 3 % if NO_x emissions are reduced by 40 % (lower row of Figure 2). This is due to competition between HNO_3 and H_2SO_4 to react with NH_3 and form particles, i.e.

5 reducing NO_x emissions means NH_3 is more readily available to react with H_2SO_4. The positive values of RCs of SO_4^{2-} to SO_2 emissions are geographically fairly uniform (somewhat lower sensitivity in the eastern UK), but the relative sensitivity to NH_3 emissions is more heterogeneous and greater in the east.

The sensitivity of particulate NO_3^- concentrations to the emissions is more straightforward than for particulate NH_4^+ and SO_4^{2}, being dominated by its positive sensitivity to NO_x emissions, weakly sensitive to NH_3 emissions and essentially not sensitive

10 at all to SO_2 emissions (Figure 1 and middle row of Figure 2). The sensitivity to NO_x emissions is almost unity, such that for example a 30 % reduction in NO_x emissions results in almost the same 30 % reduction in surface NO_3^-. The spatial distribution of RCs that represent sensitivity of NO_3^- concentrations to NO_x (and NH_3) emissions is also geographically more homogenous across the UK than the sensitivities of NH_4^+ and SO_4^{2-} concentrations (middle row of Figure 2).

The concentrations of the three inorganic particulate matter components are determined by the reactions that lead to formation

15 of $(NH_4)_2SO_4$ and NH_4NO_3. Formation of the former is irreversible whilst the latter exists in reversible equilibrium with gas-phase NH_3 and HNO_3. Changes in emissions of NH_3 have an impact on formation of both $(NH_4)_2SO_4$ and NH_4NO_3 very quickly, and therefore close to the source of the NH_3 emissions, because it reacts directly as NH_3. In contrast the influence of changes in SO_2 and NO_x emissions is not so localised. Before they influence the formation of $(NH_4)_2SO_4$ and NH_4NO_3 these gases must be oxidised in the atmosphere to H_2SO_4 and HNO_3, during which time the air is undergoing transport. The spatial

20 pattern of the sensitivities of $(NH_4)_2SO_4$ and NH_4NO_3 formation to changes in the UK precursor emissions is therefore the outcome of many interacting factors: i) the magnitude of background import of precursors from outside the UK which could explain lower sensitivity of inorganic particulate matter components to SO_2 emissions in south-east England, ii) the magnitude and spatial pattern of the UK precursors, iii) the time taken for chemical oxidation in relation to atmospheric transport of air masses, and iv) the varying dry and wet deposition spatial patterns that remove from the atmosphere both the precursor gases

25 and particulate products.

In summary, the broad patterns of the sensitivity results in Figures 1, 2 and 3 can be explained as follows. The surface concentrations of the directly emitted pollutants NH_3, NO_x and SO_2 are predominantly sensitive only to their respective emissions (Figure 1). This is also the case for the deposition of oxidised S, and of oxidised and reduced N. Dry deposition is dominated by the gas-phase components so the variations in the dry deposition of NH_x and SO_y are dominated by the variations

30 in the emissions of NH_3 and SO_x respectively with the RC values being close to 1. For the dry deposition of NO_y, both NO_2 and its oxidation product HNO_3 are important. This is illustrated by the weaker response of dry NO_y deposition to changes in NO_x emissions. Wet deposition is a more complex process as this is dominated by washout of the particles which are the product of chemical reactions in the atmosphere. This explains lower values of RC for wet compared to dry deposition.

The considerably more ubiquitous sources of NO_x emissions compared with SO_2 emissions means that atmospheric concentrations of gaseous oxidised N are generally higher than for oxidised S so the former usually has greater influence on NH_3 chemistry. Therefore particulate NO_3^- is predominantly controlled by NO_x emissions, and changes in SO_2 emissions have very little effect on particulate NO_3^-. However, because lower NO_x emissions lead to lower NH_4NO_3 formation more NH_3 is available which means lower NO_x emissions leads to greater $(NH_4)_2SO_4$ formation this explains the inverse correlation between surface concentrations of SO_4^{2-} and NO_x emissions. On the other hand, changes in NH_3 emissions impact on both NO_3^- and SO_4^{2-} concentrations, both in a positive direction of association, but with a magnitude sensitive to the relative amounts of the reacting species present, which in turn depends both on the magnitudes and distances of local sources and on long-range transport. Likewise, the sensitivity of NH_4^+ concentrations varies with all three sets of precursor emissions and with geographical location. The same is the case for concentrations of HNO_3. This is why, aside from some broad expectations, it is not easily possible to predict the spatial patterns of the sensitivities of ACTM model output to changes in emissions and a formal sensitivity analysis is needed.

3.2 Uncertainty propagation

The global uncertainty propagation approach for FRAME output variables was based on the assigned uncertainties in the estimates of the total UK emissions of SO_2 ($\pm$ 4 %), NO_x ($\pm$ 10 %) and NH_3 ($\pm$ 20 %) (Misra et al., 2015). As explained in the Methods, the uncertainties in the input emissions were assigned uniform distributions, and no uncertainties in either the spatial or temporal aspects of the emissions are included. No substantial difference in the resulting model output uncertainty ranges was observed when the probability distributions of the input emissions were changed to normal. The distributions of the relative uncertainties across all model grid cells for each output are shown in Figure 4. Example maps of the spatial distributions of the relative uncertainties from Figure 4 for surface concentrations of particulate NH_4^+, NO_3^-, and SO_4^{2-} and for dry and wet deposition of SO_y are shown in Figure 5. Equivalent maps for the relative uncertainties of the other FRAME output variables are shown in Supplementary Information Figure S5.
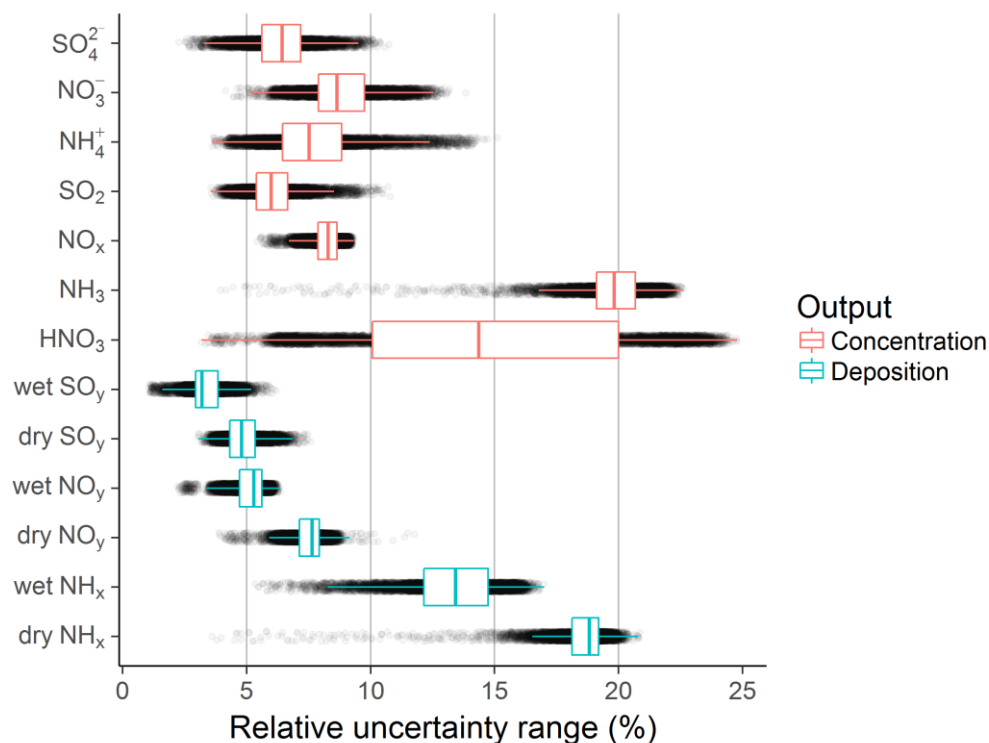
Figure 4 Distributions of relative uncertainty values calculated for all FRAME model outputs across all model grid squares given the following input uncertainty ranges: ± 4 %, ± 10 % and ± 20 % in emissions of SO_2, NO_x and NH_3 respectively. Boxes demarcate the median and lower and upper quartiles of the distributions; whiskers extend to 1.5 times the interquartile range.
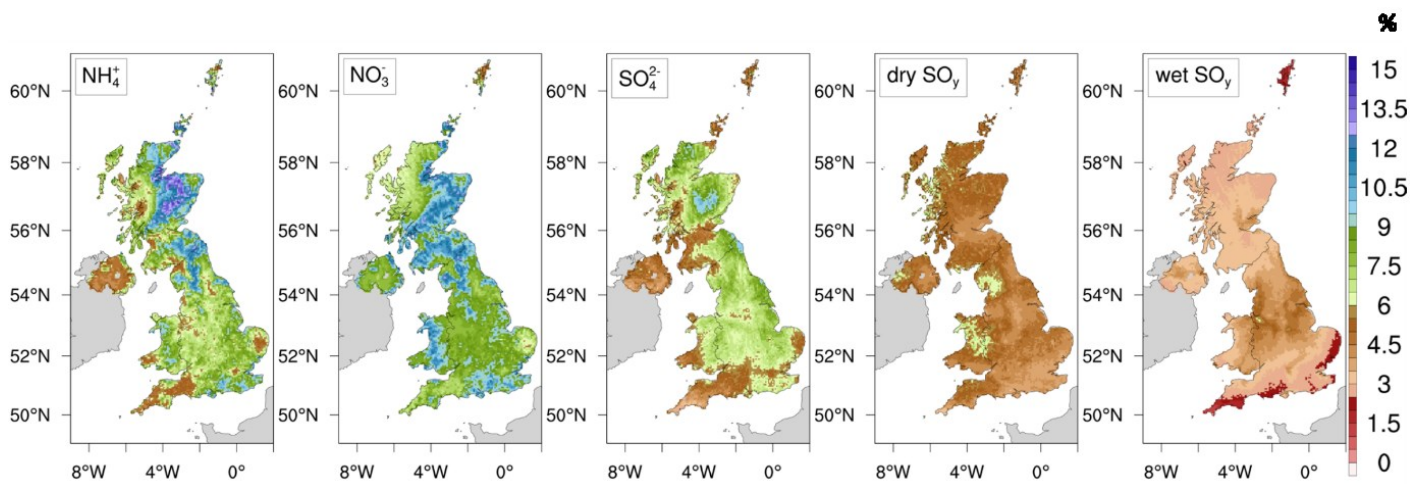
Figure 5 Spatial distributions (at the 5 km × 5 km model grid resolution) of the relative uncertainties in surface concentrations of particulate NH_4^+, SO_4^{2-}, and NO_3^- and dry and wet deposition of SO_y for uncertainties of ± 4 %, ± 10 %, ± 20 % in emissions of SO_2, NO_x and NH_3 respectively. The uncertainty values are represented as a range of +/- the baseline value and represent the 95 % confidence interval.

Figure 4 shows that the surface concentration of NH_3 is the most uncertain output (model grid median uncertainty 19.8 %). This is because the variation in NH_3 surface concentrations is almost entirely driven by variation in NH_3 input emissions (Figure 1) and this is the most uncertain input in the presented analysis. The uncertainty in modelled dry deposition of NH_x likewise closely matches the assigned uncertainty in NH_3 emissions (median = 18.8 %). The uncertainty in wet deposition of

5   NH_x is somewhat less than uncertainty in dry deposition (median = 13.4 %) because wet deposition of NH_x includes some dissolved $(NH_4)_2SO_4$ component which is also sensitive to other precursor emissions whose uncertainty is estimated to be smaller than for NH_3. Surface concentrations of SO_2 and the dry and wet depositions of SO_y have least uncertainty (medians of 6.0 %, 4.8 % and 3.2 %) for the similar reason that these model outputs are predominantly sensitive to SO_2 emissions (Figure 1) which has the smallest of the input uncertainties (± 4 %).

10   Relative uncertainties of particulate SO_4^{2-} (median = 6.4 %), NO_3^- (median = 8.6 %) and NH_4^+ (median = 7.5 %) are fairly similar (Figure 4) even though there are substantial differences in the assigned uncertainties for emissions of SO_2, NO_x and NH_3. The explanation is that PM components are sensitive to all three inputs (for NO_3^- two out of three inputs) (Figure 1). There is also wide spatial variation in the uncertainties of these PM components (Figures 4 and 5). The relative uncertainty values in surface concentration of HNO_3 show the largest variability out of all output variables. This can be explained by the

15   fact that the concentration of this species is impacted directly by both gas and particle-phase processes. The spatial pattern of the relative uncertainty values does not correlate either with the spatial pattern of emissions or rainfall, which demonstrates again that the uncertainties of many model outputs cannot be readily predicted because of the complexity of the atmospheric processes underpinning them and consequently that formal uncertainty analysis needs to be applied.

3.2.1 Uncertainty apportionment

20   Estimated uncertainty of the model output given the uncertainties in model input emissions is presented in Figures 4 and 5, but it is also of interest to know how each of the inputs contributes to the overall uncertainty individually. This was estimated by calculating squared standardised regression coefficients (SRCs) (Eq. 3). As an example, Figure 6 illustrates the spatial distributions of the fractional contributions of the SO_2, NO_x and NH_3 emission uncertainties to the overall uncertainties in surface concentrations of particulate NH_4^+, NO_3^- and SO_4^{2-}, for the assigned uncertainties in the input emissions, whilst Figure

25   7 illustrates similar for the dry and wet deposition of SO_y. The equivalent maps for the other model output variables are presented in Supplementary Information Figures S6 and S7.

Figure 6 shows that across nearly all the UK, uncertainty in concentrations of particulate NH_4^+ is mainly driven by the uncertainty in NH_3 emissions. Uncertainty in NO_x emissions contributes some uncertainty to NH_4^+ concentrations, whilst the uncertainty in SO_2 emissions makes almost no contribution. Northern Ireland is an exception; here uncertainties in NO_x

30   emissions contribute the most to the uncertainties in NH_4^+ concentrations and perturbations in NH_3 emissions have less impact. Concentrations of NH_3 in Northern Ireland are some of the highest anywhere in the UK, whilst NO_x emissions are not high; this means that NH_3 will be in excess so the formation of NH_4NO_3 will be largely controlled by HNO_3 through NO_x emissions. The major contribution to uncertainty in particulate NO_3^- derives from uncertainty in NO_x emissions (Figure 6). However in

the east of Scotland, uncertainty in NH_3 emissions contributes up to 78% of the total uncertainty. There is no contribution from SO_2 emissions uncertainty. An important feature of the lower panel of Figure 6 is that by far the major contributor to uncertainty in particulate SO_4^{2-} concentrations is the uncertainty assigned to the NH_3 emissions not the uncertainty in the direct precursor SO_2 emissions. This is because the formation of $(NH_4)_2SO_4$ is irreversibly dependent on gaseous NH_3 and emissions of NH_3 are much more uncertain than SO_2 emissions.

Figure 7 shows the spatial distribution of the squared SRC values for dry and wet SO_y deposition; for these output variables uncertainty in NO_x does not make any contribution to uncertainty in either case. In contrast to the situation for particulate SO_4^{2-} concentrations shown in Figure 6, Figure 7 shows that uncertainty in dry and wet deposition of SO_y is mainly driven by the uncertainty in the SO_2 emissions. Additionally uncertainty in NH_3 emissions contributes to the total uncertainty in dry and wet SO_y deposition. The contribution to uncertainty in wet deposition is higher due to wet deposition being dominated by the washout of the particles which include products of the reactions of NH_3 with oxidation products of SO_x.
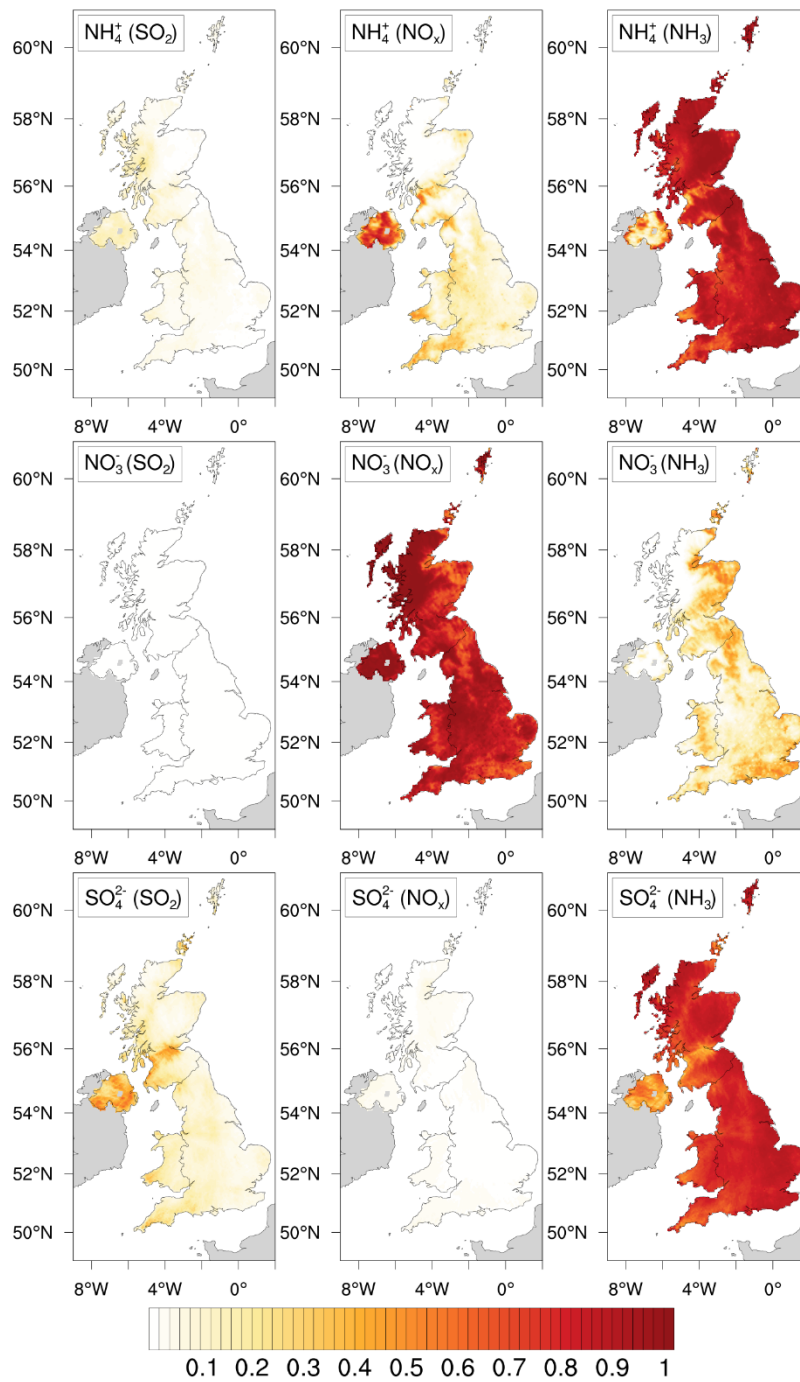
Figure 6 Spatial distributions (at the 5 km × 5 km model grid resolution) of the squared SRC values which represent the fractional contribution of the uncertainty in the input emissions given in brackets to the overall uncertainty in the surface concentrations of particulate NH_4^+, SO_4^{2-}, and NO_3^-. The uncertainties in the input emissions are ± 4 %, ± 10 % and ± 20 % for SO_2, NO_x and NH_3 respectively.
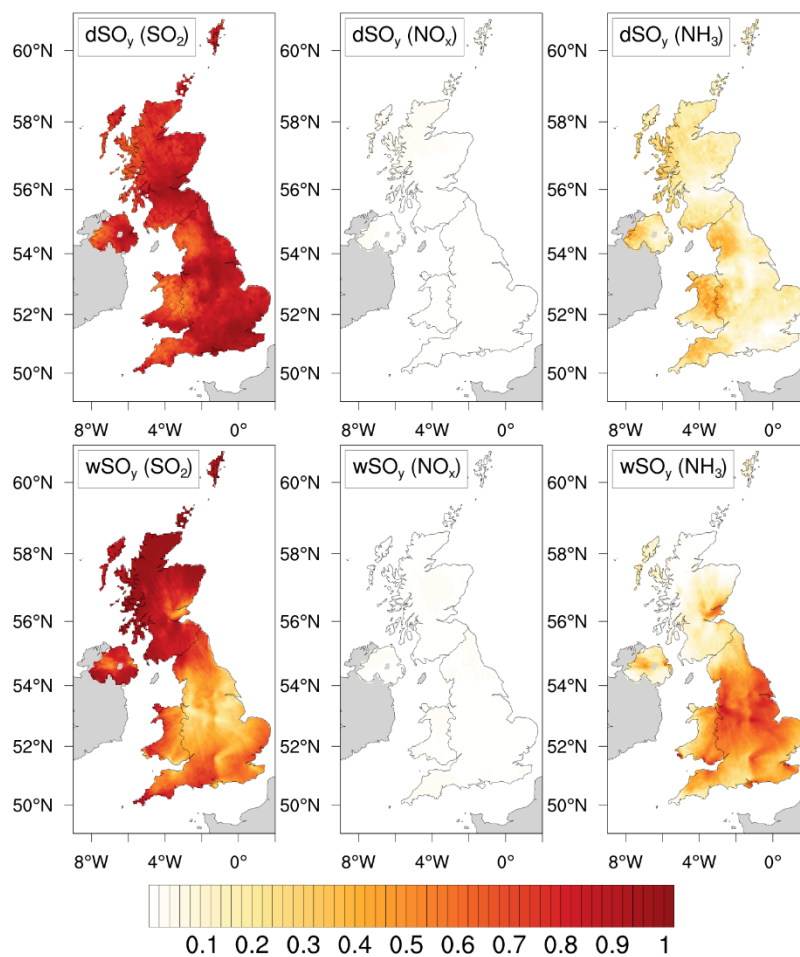
Figure 7 Spatial distributions (at the 5 km × 5 km model grid resolution) of the squared SRC values which represent the fractional contribution of the uncertainty in the input emissions given in brackets to the overall uncertainty in the dry and wet deposition of SO$_y$. The uncertainties in the input emissions are ± 4 %, ± 10 % and ± 20 % for SO$_2$, NO$_x$ and NH$_3$ respectively.

4 Conclusions

We have applied global sensitivity analysis to determine the response of concentration and deposition output variables of the FRAME atmospheric chemistry transport model to perturbations of UK emissions of SO$_2$, NO$_x$ and NH$_3$. The benefit of using systematic global sensitivity analysis is that all dimensions of variable input space are investigated simultaneously, which is important when the response to a large number of variables is of interest, so inferences can be drawn without assumptions about the model structure. For complex models such as ACTMs, for which input-output mapping is not analytically tractable,

it is not possible to predict output sensitivities to multiple input perturbations without conducting a global sensitivity analysis. Local one-at-a-time sensitivity analysis is often applied without acknowledging the shortcomings associated with it.

In this study no substantial deviations from linearity or presence of interactions between the model input variables were identified for the FRAME model in response to input emission perturbations within a ±40 % range, hence regression coefficients obtained from multiple linear regression were chosen as a sensitivity measure. This was not predictable from a local one-at-a-time sensitivity analysis.

Whilst sensitivity of surface concentrations of the primary precursor gases SO_2, NO_x and NH_3 (and of deposition of S and N) was dominated by the emissions of the respective pollutant, the sensitivities of secondary species such as HNO_3 and particulate SO_4^{2-}, NO_3^- and NH_4^+ to pollutant emissions were more nuanced and geographically variable. The dry deposition of S and N showed stronger response to changes in the emissions of the respective pollutant compared to wet deposition.

A global uncertainty analysis approach was used to estimate uncertainty ranges for all FRAME model output variables from the uncertainties assigned to the UK emissions of SO_2, NO_x and NH_3 (± 4 %, ± 10 % and ± 20 % respectively) by the UK National Atmospheric Emissions Inventory. The spatial distribution of the relative uncertainty was affected by both the sensitivity of the model output to variations in the inputs and the magnitude of this variation (i.e. the input uncertainty range); NH_3 was the most uncertain input and as a result the output variables sensitive to NH_3 showed the highest levels of relative uncertainty in the areas most sensitive to this input. The uncertainty in the surface concentrations of NH_3 and NO_x and the depositions of NH_x and NO_y was shown to be due to uncertainty in a single precursor input variable, NH_3 and NO_x respectively. In contrast, the concentration of SO_2 and deposition of SO_y was affected by uncertainties in both SO_2 and NH_3 emissions. Likewise, the relative uncertainties in the modelled surface concentrations of each of the secondary pollutant variables (NH_4^+, NO_3^-, SO_4^{2-}, and HNO_3) were affected by the uncertainty range of at least two input variables.

This work has demonstrated a methodology for conducting global sensitivity and uncertainty analysis for ACTMs. Although, for the FRAME model used here, the response to emission perturbations was found to be substantially linear in the investigated input range, the complexity of chemical and physical processes included in ACTMs means that the input-output relationships, in particular their spatial patterns, cannot be predicted without conducting a global sensitivity analysis. The benefit of using global approaches is that all dimensions of input variable space are investigated simultaneously so model input-output relationships can be quantified without the need to make strong prior assumptions about the model response to perturbations in the inputs of interest.

Data availability

The FRAME model code is not available in the public domain as the model is the intellectual property of the Centre for Ecology & Hydrology and is only made available to students and researchers who are collaborating directly with CEH staff. However, all the following output data are available at: https://doi.org/10.5281/zenodo.1145852.

1) All FRAME model outputs (raw data) for both actual input uncertainty and ± 40 % input ranges.

2) R scripts used to calculate RCs, SRCs, and uncertainty ranges.

3) Calculated RCs, SRCs, and uncertainty ranges for every FRAME output variable, which underpin all figures in this paper.

Competing interests

5 The authors declare they have no competing interests.

Acknowledgements

K. Aleksankina acknowledges studentship funding from the University of Edinburgh and the NERC Centre for Ecology & Hydrology (NERC CEH project number NEC05006). The CEH funding was provided by the Department for Environment Food & Rural Affairs contract AQ0947 Support for National Air Pollution Control Strategies 2013-2015 (SNAPS).

10 **References**

Appel, K. W., Gilliland, A. B., Sarwar, G. and Gilliam, R. C.: Evaluation of the Community Multiscale Air Quality (CMAQ) model version 4.5: Sensitivities impacting model performance, Atmos. Environ., 41(40), 9603–9615, doi:10.1016/j.atmosenv.2007.08.044, 2007.

AQEG: Linking Emission Inventories and Ambient Measurements. [online] Available from: https://uk-
15 air.defra.gov.uk/assets/documents/reports/cat11/1508060906_DEF-
PB14106_Linking_Emissions_Inventories_And_Ambient_Measurements_Final.pdf, 2015.

Bergin, M. S., Noblet, G. S., Petrini, K., Dhieux, J. R., Milford, J. B. and Harley, R. A.: Formal Uncertainty Analysis of a Lagrangian Photochemical Air Pollution Model, Environ. Sci. Technol., 33(7), 1116–1126, doi:10.1021/es980749y, 1999.

Blatman, G. and Sudret, B.: A comparison of three metamodel-based methods for global sensitivity analysis: GP modelling,
20 HDMR and LAR-gPC, Procedia - Soc. Behav. Sci., 2(6), 7613–7614, doi:10.1016/j.sbspro.2010.05.143, 2010.

Boldo, E., Linares, C., Lumbreras, J., Borge, R., Narros, A., García-Pérez, J., Fernández-Navarro, P., Pérez-Gómez, B., Aragonés, N., Ramis, R., Pollán, M., Moreno, T., Karanasiou, A. and López-Abente, G.: Health impact assessment of a reduction in ambient PM2.5 levels in Spain, Environ. Int., 37(2), 342–348, doi:10.1016/j.envint.2010.10.004, 2011.

Borge, R., Alexandrov, V., José del Vas, J., Lumbreras, J. and Rodríguez, E.: A comprehensive sensitivity analysis of the WRF
25 model for air quality applications over the Iberian Peninsula, Atmos. Environ., 42(37), 8560–8574, doi:10.1016/j.atmosenv.2008.08.032, 2008.

Box, G. E. P. and Hunter, J. S.: The 2 k-p Fractional Factorial Designs Part I, Technometrics, 3(3), 311–351, doi:10.2307/1266725, 1961.

Capaldo, K. P. and Pandis, S. N.: Dimethylsulfide chemistry in the remote marine atmosphere: Evaluation and sensitivity analysis of available mechanisms, J. Geophys. Res.-Atmos., 102(D19), 23251–23267, doi:10.1029/97JD01807, 1997.

Carnell, R.: lhs: Latin Hypercube Samples, [online] Available from: https://cran.r-project.org/package=lhs, 2016.

Carslaw, K. S., Lee, L. A., Reddington, C. L., Pringle, K. J., Rap, A., Forster, P. M., Mann, G. W., Spracklen, D. V.,

5   Woodhouse, M. T., Regayre, L. A. and Pierce, J. R.: Large contribution of natural aerosols to uncertainty in indirect forcing, Nature, 503(7474), 67–71, doi:10.1038/nature12674, 2013.

Chen, S., Brune, W. H., Lambe, A. T., Davidovits, P. and Onasch, T. B.: Modeling organic aerosol from the oxidation of α-pinene in a Potential Aerosol Mass (PAM) chamber, Atmos. Chem. Phys., 13(9), 5017–5031, doi:10.5194/acp-13-5017-2013, 2013.

10   Christian, K. E., Brune, W. H. and Mao, J.: Global sensitivity analysis of the GEOS-Chem chemical transport model: ozone and hydrogen oxides during ARCTAS (2008), Atmos. Chem. Phys., 17(5), 3769–3784, doi:10.5194/acp-17-3769-2017, 2017.

Crippa, M., Janssens-Maenhout, G., Dentener, F., Guizzardi, D., Sindelarova, K., Muntean, M., Van Dingenen, R. and Granier, C.: Forty years of improvements in European air quality: regional policy-industry interactions with global impacts, Atmos. Chem. Phys., 16(6), 3825–3841, doi:10.5194/acp-16-3825-2016, 2016.

15   Dean, A., Morris, M., Stufken, J. and Bingham, D.: Handbook of Design and Analysis of Experiments, Chapman and Hall/CRC, New York., 2015.

Derwent, R. G.: Treating uncertainty in models of the atmospheric chemistry of nitrogen compounds, Atmos. Environ., 21(6), 1445–1454, doi:10.1016/0004-6981(88)90095-9, 1987.

Dore, A. J., Kryza, M., Hall, J. R., Hallsworth, S., Keller, V. J. D., Vieno, M. and Sutton, M. a.: The influence of model grid

20   resolution on estimation of national scale nitrogen deposition and exceedance of critical loads, Biogeosciences, 9(5), 1597–1609, doi:10.5194/bg-9-1597-2012, 2012.

Dore, A. J., Carslaw, D. C., Braban, C., Cain, M., Chemel, C., Conolly, C., Derwent, R. G., Griffiths, S. J., Hall, J., Hayman, G., Lawrence, S., Metcalfe, S. E., Redington, A., Simpson, D., Sutton, M. A., Sutton, P., Tang, Y. S., Vieno, M., Werner, M. and Whyatt, J. D.: Evaluation of the performance of different atmospheric chemical transport models and inter-comparison of

25   nitrogen   and   sulphur   deposition   estimates   for   the   UK,   Atmos.   Environ.,   119(606),   131–143, doi:10.1016/j.atmosenv.2015.08.008, 2015.

Fournier, N., Pais, V. A., Sutton, M. A., Weston, K. J., Dragosits, U., Tang, S. Y. and Aherne, J.: Parallelisation and application of a multi-layer atmospheric transport model to quantify dispersion and deposition of ammonia over the British Isles, Environ. Pollut., 116(1), 95–107, doi:10.1016/S0269-7491(01)00146-4, 2002.

30   Fournier, N., Dore, a. J., Vieno, M., Weston, K. J., Dragosits, U. and Sutton, M. a.: Modelling the deposition of atmospheric oxidised nitrogen and sulphur to the United Kingdom using a multi-layer long-range transport model, Atmos. Environ., 38(5), 683–694, doi:10.1016/j.atmosenv.2003.10.028, 2004.

Frost, G. J., Middleton, P., Tarrasón, L., Granier, C., Guenther, A., Cardenas, B., Denier van der Gon, H., Janssens-Maenhout, G., Kaiser, J. W., Keating, T., Klimont, Z., Lamarque, J. F., Liousse, C., Nickovic, S., Ohara, T., Schultz, M. G., Skiba, U.,

Van Aardenne, J. and Wang, Y.: New Directions: GEIA's 2020 vision for better air emissions information, Atmos. Environ., 81(2013), 710–712, doi:10.1016/j.atmosenv.2013.08.063, 2013.

Hanna, S. R., Paine, R., Heinold, D., Kintigh, E. and Baker, D.: Uncertainties in air toxics calculated by the dispersion models AERMOD and ISCST3 in the Houston ship channel area, J. Appl. Meteorol. Climatol., 46(9), 1372–1382, doi:10.1175/JAM2540.1, 2007.

Heal, M. R., Heaviside, C., Doherty, R. M., Vieno, M., Stevenson, D. S. and Vardoulakis, S.: Health burdens of surface ozone in the UK for a range of future scenarios, Environ. Int., 61, 36–44, doi:10.1016/j.envint.2013.09.010, 2013.

Hellsten, S., Dragosits, U., Place, C. J., Vieno, M., Dore, A. J., Misselbrook, T. H., Tang, Y. S. and Sutton, M. A.: Modelling the spatial distribution of ammonia emissions in the UK, Environ. Pollut., 154(3), 370–379, doi:10.1016/j.envpol.2008.02.017, 2008.

Homma, T. and Saltelli, A.: Importance measures in global sensitivity analysis of nonlinear models, Reliab. Eng. Syst. Saf., 52(1), 1–17, doi:10.1016/0951-8320(96)00002-6, 1996.

IPCC: IPCC Guidelines for National Greenhouse Gas Inventories, General Guidance and Reporting. [online] Available from: https://www.ipcc-nggip.iges.or.jp/public/2006gl/pdf/1_Volume1/V1_3_Ch3_Uncertainties.pdf, 2006.

Jimenez, L. O. and Landgrebe, D.: Supervised classification in high-dimensional space: geometrical, statistical, and asymptotical properties of multivariate data, IEEE Trans. Syst. Man Cybern. Part C, 28(1), 39–54, doi:10.1109/5326.661089, 1998.

Johnson, M. E., Moore, L. M. and Ylvisaker, D.: Minimax and maximin distance designs, J. Stat. Plan. Inference, 26(2), 131–148, doi:10.1016/0378-3758(90)90122-B, 1990.

Konda, U., Singh, T., Singla, P. and Scott, P.: Uncertainty propagation in puff-based dispersion models using polynomial chaos, Environ. Model. Softw., 25(12), 1608–1618, doi:10.1016/j.envsoft.2010.04.005, 2010.

Labrador, L. J., von Kuhlmann, R. and Lawrence, M. G.: The effects of lightning-produced NO_x and its vertical distribution on atmospheric chemistry: sensitivity simulations with MATCH-MPIC, Atmos. Chem. Phys., 5(7), 1815–1834, doi:10.5194/acp-5-1815-2005, 2005.

Lagerwall, G., Kiker, G., Muñoz-Carpena, R. and Wang, N.: Global uncertainty and sensitivity analysis of a spatially distributed ecological model, Ecol. Modell., 275, 22–30, doi:10.1016/j.ecolmodel.2013.12.010, 2014.

Lee, L. A., Carslaw, K. S., Pringle, K. J., Mann, G. W. and Spracklen, D. V.: Emulation of a complex global aerosol model to quantify sensitivity to uncertain parameters, Atmos. Chem. Phys., 11(23), 12253–12273, doi:10.5194/acp-11-12253-2011, 2011.

Makar, P. A., Moran, M. D., Zheng, Q., Cousineau, S., Sassi, M., Duhamel, A., Besner, M., Davignon, D., Crevier, L.-P. and Bouchet, V. S.: Modelling the impacts of ammonia emissions reductions on North American air quality, Atmos. Chem. Phys., 9(18), 7183–7212, doi:10.5194/acp-9-7183-2009, 2009.

Makler-Pick, V., Gal, G., Gorfine, M., Hipsey, M. R. and Carmel, Y.: Sensitivity analysis for complex ecological models – A new approach, Environ. Model. Softw., 26(2), 124–134, doi:10.1016/j.envsoft.2010.06.010, 2011.

Matejko, M., Dore, A. J., Hall, J., Dore, C. J., Błaś, M., Kryza, M., Smith, R. and Fowler, D.: The influence of long term trends in pollutant emissions on deposition of sulphur and nitrogen and exceedance of critical loads in the United Kingdom, Environ. Sci. Policy, 12(7), 882–896, doi:10.1016/j.envsci.2009.08.005, 2009.

McKay, M. D., Beckman, R. J. and Conover, W. J.: Comparison of Three Methods for Selecting Values of Input Variables in the Analysis of Output from a Computer Code, Technometrics, 21(2), 239–245, doi:10.1080/00401706.1979.10489755, 1979.

Misra, A., Passant, N. R., Murrells, T. P., Pang, Y., Thistlethwaite, G., Walker, C., Broomfield, M., Wakeling, D., del Vento, S., Pearson, B., Hobson, M., Misselbrook, T. and Dragosits, U.: UK Informative Inventory Report (1990 to 2013)., 2015.

Morris, M. D. and Mitchell, T. J.: Exploratory designs for computational experiments, J. Stat. Plan. Inference, 43(3), 381–402, doi:10.1016/0378-3758(94)00035-T, 1995.

Norton, J.: An introduction to sensitivity assessment of simulation models, Environ. Model. Softw., 69, 166–174, doi:10.1016/j.envsoft.2015.03.020, 2015.

Oxley, T., Apsimon, H., Dore, A., Sutton, M., Hall, J., Heywood, E., Gonzales Del Campo, T. and Warren, R.: The UK Integrated Assessment Model , UKIAM : A National Scale Approach to the Analysis of Strategies for Abatement of Atmospheric Pollutants Under the Convention on Long-Range Transboundary Air Pollution, Integr. Assess., 4(4), 236–249, doi:10.1080/1389517049051538, 2003.

Oxley, T., Dore, A. J., ApSimon, H., Hall, J. and Kryza, M.: Modelling future impacts of air pollution using the multi-scale UK Integrated Assessment Model (UKIAM)., Environ. Int., 61, 17–35, doi:10.1016/j.envint.2013.09.009, 2013.

Park, J. S.: Optimal Latin-hypercube designs for computer experiments, J. Stat. Plan. Inference, 39(1), 95–111, doi:10.1016/0378-3758(94)90115-5, 1994.

Pulles, T. and Kuenen, J.: EMEP/EEA air pollutant emission inventory guidebook. [online] Available from: https://www.eea.europa.eu/publications/emep-eea-guidebook-2016, 2016.

Rypdal, K. and Winiwarter, W.: Uncertainties in greenhouse gas emission inventories — evaluation, comparability and implications, Environ. Sci. Policy, 4(2–3), 107–116, doi:10.1016/S1462-9011(00)00113-1, 2001.

Saltelli, A.: Making best use of model evaluations to compute sensitivity indices, Comput. Phys. Commun., 145, 280–297, doi:10.1016/S0010-4655(02)00280-1, 2002.

Saltelli, A. and Annoni, P.: How to avoid a perfunctory sensitivity analysis, Environ. Model. Softw., 25(12), 1508–1517, doi:10.1016/j.envsoft.2010.04.012, 2010.

Saltelli, A., Chan, K. and Scott, E. M.: Sensitivity Analysis, edited by A. Saltelli, K. Chan, and E. M. Scott, Wiley, Chichester, UK., 2000.

Saltelli, A., Ratto, M., Andres, T., Campolongo, F., Cariboni, J., Gatelli, D., Saisana, M. and Tarantola, S.: Global Sensitivity Analysis. The Primer, John Wiley & Sons, Ltd, Chichester, UK., 2008.

Saltelli, A., Annoni, P., Azzini, I., Campolongo, F., Ratto, M. and Tarantola, S.: Variance based sensitivity analysis of model output. Design and estimator for the total sensitivity index, Comput. Phys. Commun., 181(2), 259–270, doi:10.1016/j.cpc.2009.09.018, 2010.

Sax, T. and Isakov, V.: A case study for assessing uncertainty in local-scale regulatory air quality modeling applications, Atmos. Environ., 37(25), 3481–3489, doi:10.1016/S1352-2310(03)00411-4, 2003.

Shahsavani, D. and Grimvall, A.: Variance-based sensitivity analysis of model outputs using surrogate models, Environ. Model. Softw., 26(6), 723–730, doi:10.1016/j.envsoft.2011.01.002, 2011.

5 Shin, M. J., Guillaume, J. H. A., Croke, B. F. W. and Jakeman, A. J.: Addressing ten questions about conceptual rainfall-runoff models with global sensitivity analyses in R, J. Hydrol., 503(2013), 135–152, doi:10.1016/j.jhydrol.2013.08.047, 2013.

De Simone, F., Gencarelli, C. N., Hedgecock, I. M. and Pirrone, N.: Global atmospheric cycle of mercury: A model study on the impact of oxidation mechanisms, Environ. Sci. Pollut. Res., 21(6), 4110–4123, doi:10.1007/s11356-013-2451-x, 2014.

Simpson, D., Tuovinen, J. P., Emberson, L. and Ashmore, M. R.: Characteristics of an ozone deposition module II: Sensitivity

10 analysis, Water. Air. Soil Pollut., 143(1–4), 123–137, doi:10.1023/A:1022890603066, 2003.

Singles, R., Sutton, M. A. and Weston, K. J.: A multi-layer model to describe the atmospheric transport and deposition of ammonia in Great Britain, Atmos. Environ., 32(3), 393–399, doi:10.1016/S1352-2310(97)83467-X, 1998.

Skamarock, W., Klemp, J., Dudhia, J., Gill, D., Barker, D., Duda, M., Huang, X., Wang, W. and Powers, J.: A Description of the Advanced Research WRF Version 3. NCAR technical note NCAR/TN-475+STR., 2008.

15 Sobol', I. M.: On the distribution of points in a cube and the approximate evaluation of integrals, USSR Comput. Math. Math. Phys., 7(4), 86–112, doi:10.1016/0041-5553(67)90144-9, 1967.

Sobol', I. M.: Uniformly distributed sequences with an additional uniform property, USSR Comput. Math. Math. Phys., 16(5), 236–242, doi:10.1016/0041-5553(76)90154-3, 1976.

Sobol', I. M.: Sensitivity analysis for non-linear mathematical models, Math. Model. Comput. Exp., 1(4), 407–414, 1993.

20 Sobol', I. M. and Levitan, Y. L.: A pseudo-random number generator for personal computers, Comput. Math. with Appl., 37(4–5), 33–40, doi:10.1016/S0898-1221(99)00057-7, 1999.

Song, X., Bryan, B. A., Paul, K. I. and Zhao, G.: Variance-based sensitivity analysis of a forest growth model, Ecol. Modell., 247, 135–143, doi:10.1016/j.ecolmodel.2012.08.005, 2012.

Storlie, C. B. and Helton, J. C.: Multiple predictor smoothing methods for sensitivity analysis: Description of techniques,

25 Reliab. Eng. Syst. Saf., 93(1), 28–54, doi:10.1016/J.RESS.2006.10.012, 2008.

Thompson, T. M. and Selin, N. E.: Influence of air quality model resolution on uncertainty associated with health impacts, Atmos. Chem. Phys., 12(20), 9753–9762, doi:10.5194/acp-12-9753-2012, 2012.

United Nations Economic Commission for Europe: Guidelines for Reporting Emissions and Projections Data under the Convention on Long-range Transboundary Air Pollution. [online] Available from:

30 https://www.unece.org/fileadmin/DAM/env/documents/2015/AIR/EB/English.pdf, 2015.

Vieno, M., Heal, M. R., Williams, M. L., Carnell, E. J., Nemitz, E., Stedman, J. R. and Reis, S.: The sensitivities of emissions reductions for the mitigation of UK PM 2.5, Atmos. Chem. Phys., 16(1), 265–276, doi:10.5194/acp-16-265-2016, 2016.

Xing, J., Wang, S. X., Chatani, S., Zhang, C. Y., Wei, W., Hao, J. M., Klimont, Z., Cofala, J. and Amann, M.: Projections of air pollutant emissions and its impacts on regional air quality in China in 2020, Atmos. Chem. Phys., 11(7), 3119–3136,

doi:10.5194/acp-11-3119-2011, 2011.

Yatheendradas, S., Wagener, T., Gupta, H., Unkrich, C., Goodrich, D., Schaffner, M. and Stewart, A.: Understanding uncertainty in distributed flash flood forecasting for semiarid regions, Water Resour. Res., 44(5), doi:10.1029/2007WR005940, 2008.

5   Zhang, Y., Liu, X.-H., Olsen, K. M., Wang, W.-X., Do, B. A. and Bridgers, G. M.: Responses of future air quality to emission controls over North Carolina, Part II: Analyses of future-year predictions and their policy implications, Atmos. Environ., 44(23), 2767–2779, doi:10.1016/j.atmosenv.2010.03.022, 2010.